# Identification of $Mn(CO)_nCF_3^-$ ($n$ = 4, 5) Structural Isomers by IR Multiphoton Dissociation, Collision-Induced Dissociation, and Specific Ligand Displacement Reactions: Studies of the Trifluoromethyl Migratory Decarbonylation Reaction in the Gas Phase

**Seung Koo Shin and J. L. Beauchamp***

*Contribution No. 7951 from the Arthur Amos Noyes Laboratory of Chemical Physics, California Institute of Technology, Pasadena, California 91125. Received August 9, 1989*

**Abstract:** The trifluoromethyl migratory decarbonylation reaction which converts the (trifluoroacetyl)manganese tetracarbonyl anion to the (trifluoromethyl)manganese tetracarbonyl anion is studied in the gas phase with Fourier transform ion cyclotron resonance spectroscopy. Dissociative electron attachment by (trifluoroacetyl)manganese pentacarbonyl produces both $Mn(CO)_5CF_3^-$ and $Mn(CO)_4CF_3^-$. $Mn(CO)_5CF_3^-$ slowly decomposes to yield $Mn(CO)_4CF_3^-$ with loss of CO. In order to identify the structures of these two ions, we have employed infrared multiphoton dissociation in conjunction with collision-induced dissociation and studies of specific reactivity involving the ligand displacement process. $Mn(CO)_4CF_3^-$ derived from dissociative electron attachment by a different precursor, (trifluoromethyl)manganese pentacarbonyl, is also used to confirm the identity of the trifluoromethyl-migration product ion. The $Mn(CO)_5CF_3^-$ ion generated from (trifluoroacetyl)manganese pentacarbonyl does not undergo infrared multiphoton dissociation in the $CO_2$ laser wavelength range, which indicates the trifluoroacetyl structure $CF_3COMn(CO)_4^-$. $Mn(CO)_4CF_3^-$ ions derived from the two different precursors show identical infrared multiphoton dissociation spectral features within experimental errors. Two absorption maxima at 1052 and 945 $cm^{-1}$ are assigned as a symmetric C-F stretch of $A_1$-type symmetry and a degenerate C-F stretch of E-type symmetry, respectively. Collision-induced dissociation of $Mn(CO)_4CF_3^-$ yields indistinguishable fragment mass spectra from the two different precursors. Identical rate constants within experimental error are measured for $Mn(CO)_4CF_3^-$ from the two precursors in ligand displacement reactions with NO to yield $Mn(CO)_3(NO)CF_3^-$ with loss of CO. Displacement of CO by $^{13}CO$ or $PF_3$ is not observed for either ion. These results support identical structures for $Mn(CO)_4CF_3^-$ from the two different precursors, with the $CF_3$ ligand directly bonded to manganese, $CF_3Mn(CO)_4^-$. It is postulated that this ion from (trifluoromethyl)manganese pentacarbonyl is produced directly by electron attachment accompanied by loss of one equatorial CO. With (trifluoroacetyl)manganese pentacarbonyl, electron attachment leads to loss of an equatorial CO followed by the migration of $CF_3$ from the acyl carbon to the vacant equatorial site on the manganese center with loss of another CO in the equatorial position to the $CF_3$ ligand. The $CF_3$ group is an ideal infrared chromophore to investigate the infrared photochemistry of organometallic complexes, allowing studies of the structures and reaction mechanisms of coordinatively unsaturated intermediates containing metal-bonded $CF_3$ groups.

Organometallic migration reactions have been studied extensively in recent years.[1] Many kinetic and stereochemical studies of alkyl to acyl migratory-insertion reactions have been reported. The generally accepted two-step mechanism for migratory-insertion, which is presented in eq 1, invokes a coordinatively unsaturated acyl intermediate. In the first step there is an equi-

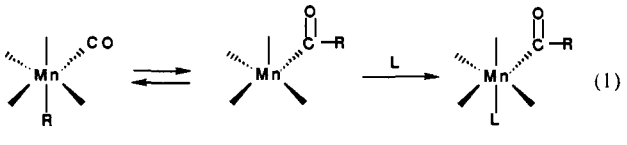


(1)

librium between the coordinatively saturated alkyl complex and the coordinatively unsaturated acyl complex. The second step involves the addition of the external ligand affording the product, a saturated acyl complex. Most of the cases have been studied under conditions whereby the equilibrium lies far to the right.

Considerable attention has been directed to determine whether these reactions proceed by CO insertion or alkyl migration,[2] with less being known about the reverse alkyl-migration step from the acyl intermediate to the alkyl complex. Direct kinetic studies of the reverse methyl-migration step have been reported by Kubota et al.[3] They prepared five-coordinated (phenylacetyl)iridium complexes (I) from the oxidative addition of phenylacetyl chlorides to *trans*-chlorobis(triphenylphosphine)dinitrogeniridium. These five-coordinated iridium complexes rearrange in solution to six-coordinated benzyl(carbonyl) complexes (II). They found that electron-withdrawing groups retard this alkyl migration. Recently,

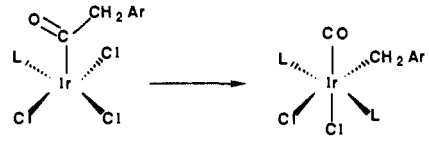


(I) (II)

Casey et al.[4] have studied reductive elimination of acetophenone from *cis*-$Mn(CO)_4(COCH_3)(COC_6H_5)^-$ (III) to measure relative migratory aptitudes between methyl and phenyl in the conversion of acyl-metal to alkyl-metal complexes. Their results were interpreted in terms of a mechanism involving loss of CO from III and formation of a five-coordinated intermediate $Mn(CO)_3(COCH_3)(COC_6H_5)^-$ (IV), which is in rapid equilibrium with a benzoylmethyl intermediate $Mn(CO)_4(CH_3)(COC_6H_5)^-$ due to the facile methyl migration. Conversion of IV to the acetylphenyl intermediate $Mn(CO)_4(COCH_3)(C_6H_5)^-$ is followed by reductive elimination to give acetophenone and $Mn(CO)_4^-$. Formation of a coordinatively unsaturated $Mn(CO)_4^-$ intermediate was confirmed by trapping with triphenylphosphine to yield $Mn(CO)_4(P(C_6H_5)_3)^-$.

(1) (a) Collman, J. P.; Hegedus, L. S. *Principles and Applications of Organotransition Metal Chemistry*; University Science Books: Mill Valley, 1980; Chapter 5. (b) Collman, J. P.; Hegedus, L. S.; Norton, J. R.; Finke, R. G. *Principles and Applications of Organotransition Metal Chemistry*; University Science Books: Mill Valley, 1987; Chapter 6.

(2) Basolo, F.; Pearson, R. G. *Mechanisms of Inorganic Reactions*, 2nd ed.; Wiley: New York, 1967; pp 578-609.

(3) Kubota, M.; Blake, D. M.; Smith, S. A. *Inorg. Chem.* **1971**, *10*, 1430.

(4) Casey, C. P.; Scheck, D. M. *J. Am. Chem. Soc.* **1980**, *102*, 2728.

0002-7863/90/1512-2057$02.50/0 

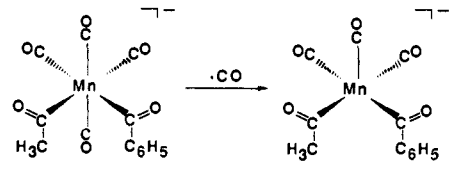

(III) (IV)

To provide a fundamental understanding of these complex organometallic reaction mechanisms, it is desirable to devise methods to isolate the coordinatively unsaturated intermediates, identify their structures, and examine the reaction kinetics in the absence of solvent effects. However, there has been no report of kinetic studies of methyl-migration reactions in the gas phase. In the present paper we employ Fourier transform ion cyclotron resonance spectroscopy to isolate the coordinatively unsaturated intermediates and examine structures, reactivities, and spectroscopic properties of the isolated intermediates for one such reaction.

Dissociative electron attachment[5] by (trifluoroacetyl)manganese pentacarbonyl, $CF_3COMn(CO)_5$, generates $Mn(CO)_5CF_3^-$ and $Mn(CO)_4CF_3^-$. The former ion is considered to be the 17 $e^-$ (trifluoroacetyl)manganese tetracarbonyl anion (V), $CF_3CO$-$Mn(CO)_4^-$, with the possibility of a 19 $e^-$ (trifluoromethyl)manganese pentacarbonyl anion, $CF_3Mn(CO)_5^-$, being considered unlikely. However, $Mn(CO)_4CF_3^-$ affords the possibility of being either trifluoroacetyl (VI) or trifluoromethyl (VII) manganese ions of the same mass-to-charge ratio. $Mn(CO)_5CF_3^-$ slowly decomposes to yield $Mn(CO)_4CF_3^-$ with loss of CO, presenting the possibility of observing the trifluoromethyl migratory decarbonylation reaction, if $Mn(CO)_5CF_3^-$ and $Mn(CO)_4CF_3^-$ have structures V and VII, respectively.

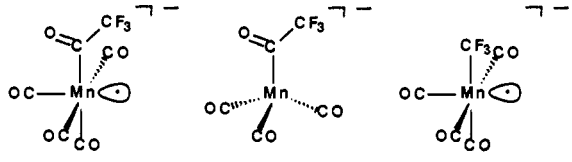

(V) (VI) (VII)

Since (trifluoromethyl)manganese pentacarbonyl, $CF_3Mn(CO)_5$, also produces $Mn(CO)_4CF_3^-$ by dissociative electron attachment, studies of $Mn(CO)_4CF_3^-$ ions derived from the two different precursors, $CF_3COMn(CO)_5$ and $CF_3Mn(CO)_5$ can be directly compared. $Mn(CO)_4CF_3^-$ obtained from the $CF_3Mn(CO)_5$ is considered to be the trifluoromethyl tetracarbonyl anion, $CF_3Mn(CO)_4^-$ (VII), because migration of $CF_3$ from $CF_3Mn(CO)_4^-$ to a carbonyl carbon yielding $CF_3CO$-$Mn(CO)_3^-$ is estimated to be endothermic by 33 kcal/mol.[6]

The structural differentiation between isomeric ions with the same mass-to-charge ratio has been explored by using several mass spectrometric techniques. These approaches, which are successful with certain classes of ions, include collision-induced dissociation (CID),[7] specific reactivity in bimolecular processes,[8] and photodissociation.[9]

The most widely used technique is high-energy collision-induced dissociation of a mass-selected ion, which often yields a characteristic fragmentation pattern useful for distinguishing isomeric structures. For example, Peake et al.[10] have probed the structures of $FeC_nH_{2n}^+$ species formed by reaction of $Fe(CO)^+$ with olefins ($n$ = 2–14) and cycloalkanes ($n$ = 3–6) using high-energy collision-induced dissociation of the iron–olefin complex in a tandem mass spectrometer (MS/MS). Freiser and co-workers[11] have utilized collision-induced dissociation techniques to distinguish isomeric structures, generate unprecedented ions, and deduce reaction mechanisms and thermochemistry for organometallic intermediates.

The second method utilizes distinguishable reactivities of isomeric ions in low-energy bimolecular ion–molecule collisions. Small hydrocarbon ions have been successfully investigated with this method.[8] In studies of organometallic intermediates, Halle et al.[12] have distinguished a bisethylene complex, $Ni(C_2H_4)_2^+$, formed by dehydrogenation of $n$-butane with $Ni^+$, from a metallacycle complex, $NiC_4H_8^+$, yielded from decarbonylation of cyclopentanone with $Ni^+$, by the different reaction products resulting from the interaction of these isomeric complexes with HCN. As another example, Jacobson and Freiser[13] have probed the structures of $Rh(C_7H_6)^+$ isomers obtained from reaction of $Rh^+$ with toluene using H/D exchange reactions with $D_2$.

Isomeric ions may be differentiated if they have different photodissociation spectra or if their photoproducts differ. Energies required for cleavage of typical bonds necessitate visible or ultraviolet radiation for single-photon events, and studies in this wavelength region have been quite useful for structure elucidation of gaseous ions.[9] Recent experiments employing infrared multiphoton dissociation (IRMPD) processes[14] have also demonstrated the possibility of isomeric differentiation based on the observed IRMPD spectra.[9b] For example, $C_3F_6^+$ molecular ions formed from either perfluoropropylene or perfluorocyclopropane, which present the possibility of observing cyclic or acyclic ions of the same mass-to-charge ratio, have identical photodissociation spectra upon gated continuous wave $CO_2$ laser irradiation.[15] Wright and Beauchamp[16] have successfully differentiated between benzyl and cycloheptatrienyl anions generated from different precursors using their distinguishable infrared multiphoton electron detachment spectra. Recently, Baykut et al.[17] have observed different infrared multiphoton dissociation products from $C_4H_9O_2^+$ ions arising from different precursors. Hanratty et al.[18] have probed the potential energy surfaces for reactions of cobalt ions with $C_5H_{10}$ isomers. Infrared multiphoton dissociation of Co(1-pentene)$^+$ and Co(2-pentene)$^+$ adducts yields distinguishable photoproducts, Co-

(5) (a) Fosier, M. S.; Beauchamp, J. L. *Chem. Phys. Lett.* **1975**, *31*, 1975. (b) Woodin, R. L.; Fosier, M. S.; Beauchamp, J. L. *J. Chem. Phys.* **1980**, *72*, 4223. (c) Squires, R. R. *Chem. Rev.* **1987**, *87*, 623.

(6) Estimated from $D[(CO)_5Mn$–$COCF_3]$ = 42.9 kcal/mol, $D[(CO)_5$-$Mn$–$CF_3]$ = 48.9 kcal/mol, $D[Mn_2(CO)_9$–$CO]$ = 36 kcal/mol, and $D(C$-$F_3$–$CO)$ = 9 kcal/mol; see ref 1b, pp 240 and 368.

(7) (a) *Collision Spectroscopy*; Cooks, R. G., Ed.; Plenum: New York, 1978. (b) Cody, R. B.; Freiser, B. S. *Int. J. Mass Spectrom. Ion Phys.* **1982**, *41*, 199. (c) Cody, R. B.; Burnier, R. C.; Freiser, B. S. *Anal. Chem.* **1982**, *54*, 96. (d) Cody, R. B.; Burnier, R. C.; Cassady, C. J.; Freiser, B. S. *Anal. Chem.* **1982**, *54*, 2225.

(8) (a) Baldeschwieler, J. D. *Science* **1968**, *159*, 263. (b) Beauchamp, J. L. *Annu. Rev. Phys. Chem.* **1971**, *22*, 527. (c) Lehman, T. A.; Bursey, M. M. *Ion Cyclotron Resonance Spectrometry*; Wiley: New York, 1976. (d) Gross, M. L.; Russell, D. H.; Aerni, R. J.; Bronczyk, S. A. *J. Am. Chem. Soc.* **1977**, *99*, 3603. (e) Ausloos, P. J. *J. Am. Chem. Soc.* **1981**, *103*, 3931. (f) Jackson, J. A. A.; Lias, S. C.; Ausloos, P. J. *J. Am. Chem. Soc.* **1977**, *99*, 7515. (g) Eyler, J. R.; Campana, J. E. *Int. J. Mass Spectrom. Ion Phys.* **1983/1984**, *55*, 171. (h) Fellerolf, D. D.; Yosi, R. A.; Eyler, J. R. *Org. Mass Spectrom.* **1984**, *19*, 104.

(9) (a) Dunbar, R. C. In *Gas Phase Ion Chemistry*; Bowers, M. T., Ed.; Academic Press: New York, 1979; Vol. 2, p 181; 1984;, Vol. 3, p 130. (b) Thorne, L. R.; Beauchamp, J. L. In *Gas Phase Ion Chemistry*; Bowers, M. T., Ed.; Academic Press: New York, 1984; Vol. 3, p 42. (c) Harris, F. M.; Beynon, J. H. In *Gas Phase Ion Chemistry*; Bowers, M. T., Ed.; Academic Press: New York, 1984; Vol. 3, p 100. (d) *Molecular Ions: Spectroscopy, Structure, and Chemistry*; Miller, T. A.; Bondybey, V. E., Ed.; North-Holland Publishing: Amsterdam, 1983; p 231. (e) *Molecular Photodissociation Dynamics*; Ashfold, M. N. R., Baggott, J. E., Eds.; The Royal Society of Chemistry: London, 1987.

(10) Peake, D. A.; Gross, M. L.; Ridge, D. P. *J. Am. Chem. Soc.* **1984**, *106*, 4307.

(11) (a) Freiser, B. S. *Talanta* **1985**, *32*, 697. (b) Jacobson, D. B.; Freiser, B. S. *J. Am. Chem. Soc.* **1983**, *105*, 736. (c) Jacobson, D. B.; Freiser, B. S. *J. Am. Chem. Soc.* **1983**, *105*, 7484.

(12) Halle, L. F.; Houriet, R.; Kappes, M. M.; Staley, R. H.; Beauchamp, J. L. *J. Am. Chem. Soc.* **1982**, *104*, 6293.

(13) Jacobson, D. B.; Freiser, B. S. *J. Am. Chem. Soc.* **1984**, *106*, 1159.

(14) (a) Lupo, D. W.; Quack, M. *Chem. Rev.* **1987**, *87*, 181 and earlier references therein. (b) Bomse, D. S.; Berman, D. W.; Beauchamp, J. L. *J. Am. Chem. Soc.* **1978**, *100*, 3248. (c) Cassassa, M. P.; Bomse, D. S.; Beauchamp, J. L.; Janda, K. C. *J. Chem. Phys.* **1980**, *72*, 6805.

(15) (a) Bomse, D. S.; Berman, D. W.; Beauchamp, J. L. *J. Am. Chem. Soc.* **1981**, *103*, 3967. (b) Woodin, R. L.; Bomse, D. S.; Beauchamp, J. L. *Chem. Phys. Lett.* **1979**, *63*, 630.

(16) Wright, C. A.; Beauchamp, J. L. *J. Am. Chem. Soc.* **1981**, *103*, 6499. (b) Wright, C. A.; Beauchamp, J. L. *Chem. Phys.*, in press.

(17) Baykut, G.; Watson, C. H.; Weller, R. R.; Eyler, J. R. *J. Am. Chem. Soc.* **1985**, *107*, 8036.

(18) Hanratty, M. A.; Paulsen, C. M.; Beauchamp, J. L. *J. Am. Chem. Soc.* **1985**, *107*, 5074.

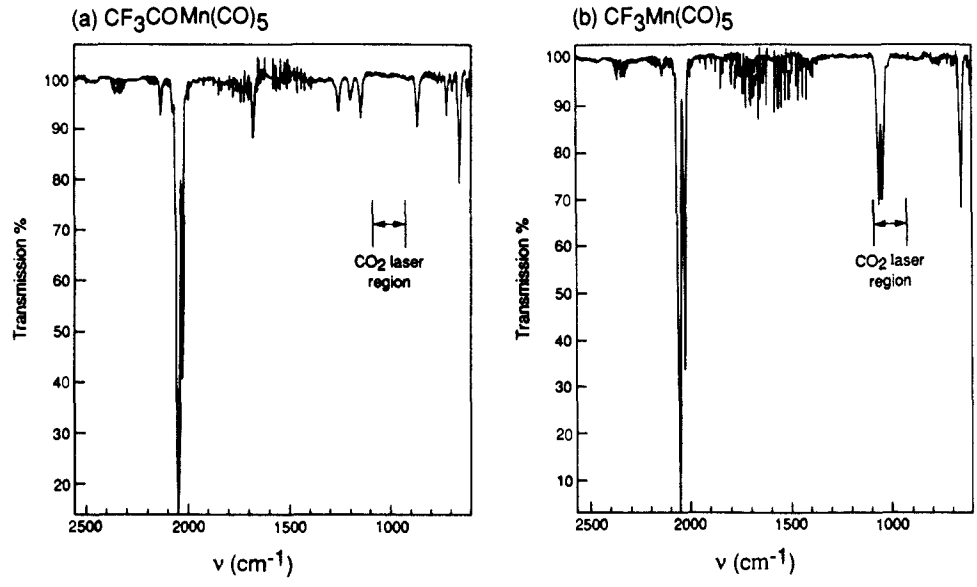


Figure 1. Gas-phase infrared absorption spectra of (trifluoroacetyl)manganese pentacarbonyl (a) and (trifluoromethyl)manganese pentacarbonyl (b). See Table I for the frequency assignment. The wavelength tuning region accessible with a $CO_2$ laser is indicated on each spectrum.

$(C_3H_6)^+$ with loss of ethylene and $Co(C_4H_6)^+$ with loss of methane, respectively, in processes that can be interpreted as resulting from the facile insertion of the metal ion into an allylic carbon–carbon bond.

In the present paper we employ infrared multiphoton dissociation, combined with FT-ICR[19] studies of collision-induced dissociation and ligand displacement processes to distinguish the structures and reactivities of $Mn(CO)_nCF_3^-$ (n = 4, 5) ions.

## Experimental Section

Experimental techniques associated with ICR spectroscopy,[8a-c] and in particular Fourier transform ion cyclotron resonance spectroscopy,[20] have been previously described in detail. Experiments were performed with use of an Ion Spec FT–ICR data system in conjunction with a 1-in. cubic trapping cell[19] built by Bio-Med Tech.[21] Experiments were carried out at 2 T with a Varian 15-in. electromagnet.

All experiments were carried out in the pressure range $10^{-8}$–$10^{-5}$ Torr, corresponding to neutral particle densities of $3.5 \times 10^9$ to $3.5 \times 10^{11}$ molecule $cm^{-3}$. Pressures were measured with a Schulz-Phelps ion gauge[22] calibrated against an MKS Baratron (Model 390 HA-0001) capacitance manometer. The principal errors in the rate constants (estimated to be ±20%) arise from uncertainties in pressure measurements.[23] Sample mixtures were prepared directly in the instrument with use of three sample inlets and the Schulz-Phelps gauge.

Where available, chemicals were obtained commercially in high purity and used as supplied except for multiple freeze–pump–thaw cycles to remove noncondensable gases. (Trifluoroacetyl)manganese pentacarbonyl, $CF_3COMn(CO)_5$, was prepared by treatment of $NaMn(CO)_5$ with trifluoroacetic anhydride. (Trifluoromethyl)manganese pentacarbonyl, $CF_3Mn(CO)_5$, was obtained by heating $CF_3COMn(CO)_5$ at 110 °C.[24] Melting points were measured on a Thomas-Hoover melting apparatus ($CF_3COMn(CO)_5$, 55–56 °C; $CF_3Mn(CO)_5$, 82–83 °C). Fluorine-19 nuclear magnetic resonance (84.57 MHz) spectra were obtained on a Jeol FX-90 spectrometer. $CF_3COMn(CO)_5$ and $CF_3Mn(CO)_5$ in benzene-$d_6$ show sharp singlets at 81.2 and 28.3 ppm downfield from $C_6F_6$, respectively.

ICR modifications for infrared photochemistry are described elsewhere.[25] The unfocused infrared beam from a grating tuned Apollo 550A CW $CO_2$ laser enters the vacuum system through an antireflection coated NaCl window (25.4 mm diameter × 3.5 mm thick) supplied by Oriel, Inc. and passes through a 92% transmittance mesh to irradiate trapped ions. The transmitter plate reflects the beam for a second pass through the ion-trapping region and out of the apparatus. Assuming that the plate reflects 100% of the incident laser beam and taking into account the 92% mesh transmittance, the beam power inside the cell is 1.84 times the power of the beam entering the vacuum system. Beam shape is monitored with an Optical Engineering Model 22A thermal imaging plate. Infrared wavelengths are measured with an Optical Engineering Model 16A spectrum analyzer. Bandwidths are estimated to be 100 MHz. Beam power is measured with a Scientech, Inc. Model 36-0001 surface absorbing disc calorimeter. Power fluctuations are typically ±5% during an experiment.

The $CO_2$ laser beam is externally triggered by the control pulse from the computer. Although laser intensity in the cell varies due to the Gaussian beam profile, irradiation of trapped ions is uniform as indicated by the fact that small translations of the laser beam do not alter photoproduct yields.

Gas-phase infrared absorption spectra of manganese compounds were recorded on a Mattson Instruments, Inc. Sirius 100 FT–IR spectrometer having a Hg–Cd–Te detector cooled by liquid $N_2$. A 10 cm path length cell equipped with NaCl windows was used.

Negative ions were generated by dissociative electron attachment, using a nominal electron beam energy of 2 eV. Since both anions and electrons are trapped in the cell during the negative-ion mode experiment, electrons are ejected from the cell shortly after the electron beam pulse by applying an oscillating electric field (about 5 $V_{pp}$ amplitude and 6.72 MHz frequency at −1 V trapping voltage) across the trapping plates. Ions formed by dissociative electron attachment are stored in the trapping ICR cell and mass-selected by a series of ion ejection pulses. Translational excitation of the reactant ion was minimized by using the lowest possible radio frequency fields. Infrared multiphoton dissociation spectra of mass-selected ions are obtained with a constant power (8 W $cm^{-2}$) and irradiation period (20 ms), which corresponds to the laser fluence of 160 mJ $cm^{-2}$, at all lines in the 925–1085 $cm^{-1}$ wavelength range. In the ligand displacement reactions of $CF_3Mn(CO)_4^-$ ions with $^{13}CO$, $PF_3$, and NO, the temporal variations of reactant and product ion abundances starting from $CF_3Mn(CO)_4^-$ were recorded and used to calculate rate constants. The ICR cell temperature is somewhat above ambient due to heating from the filament.

## Results and Discussion

**Infrared Spectra of $CF_3COMn(CO)_5$ and $CF_3Mn(CO)_5$.** Figure 1 shows gas-phase infrared absorption spectra of (trifluoroacetyl)manganese pentacarbonyl (a) and (trifluoromethyl)manganese pentacarbonyl (b). Spectrometer resolution is 0.5 $cm^{-1}$. The same samples are used for the rest of the experiments de-

(19) Comisarow, M. B. *Int. J. Mass. Spectrom. Ion Phys.* **1981**, *37*, 251.
(20) (a) *Fourier Transform Mass Spectrometry*; Buchanan, M. V. Ed.; ACS Sym. Ser. 359; American Chemical Society: Washington, DC, 1987. (b) Marshall, A. G. *Acc. Chem. Res.* **1985**, *18*, 316 and references therein.
(21) Bio-Med Tech, 2001 E. Galbreth, Pasadena, CA 91104.
(22) Schulz, G. J.; Phelps, A. V. *Rev. Sci. Instrum.* **1957**, *28*, 1051.
(23) Blint, R. J.; McMahon, T. B.; Beauchamp, J. L. *J. Am. Chem. Soc.* **1974**, *96*, 1269.
(24) (a) McClellan, W. R. *J. Am. Chem. Soc.* **1961**, *83*, 1598. (b) Coffield, T. H.; Kozikowski, J.; Closson, R. D. *Abstracts of the 5th International Conference on Coordination Chemistry, London*; The Chemical Society Special Publication 13: London, 1959; p 126. (c) King, R. B. *Organometallic Synthesis*; Academic Press: New York, 1965; Vol. 1, p 145.
(25) Bomse, D. S.; Woodin, R. L.; Beauchamp, J. L. *J. Am. Chem. Soc.* **1979**, *101*, 5503.

Table I. Infrared Frequency Assignments of $CF_3COMn(CO)_5$ and $CF_3Mn(CO)_5$

| $CF_3COMn(CO)_5$[a] | | $CF_3Mn(CO)_5$[b] | |
|---|---|---|---|
| $\nu$, $cm^{-1}$ | assignment | $\nu$, $cm^{-1}$ | assignment |
| 2134 | sym str of $(CO)_{eq}$ | 2142 | sym str of $(CO)_{eq}$ $(A_1)$ |
| 2050 | degen str of $(CO)_{eq}$ | 2055 | degen str of $(CO)_{eq}$ (E) |
| 2028 | str of $(CO)_{ax}$ | 2026 | str of $(CO)_{ax}$ $(A_1)$ |
| 1673 | str of acetyl CO | | |
| 1254 | sym str of CF | 1063 | sym str of $CF_3$ $(A_1)$ |
| 1191 | F–$CF_2$ in-plane str. | 1043 | degen str of $CF_3$ (E) |
| 1141 | F–$CF_2$ out-of-plane str. | | |
| 865 | C–C str | | |
| 719 | F–$CF_2$ deform | | |
| 650 | Mn–Co wagging | 650 | Mn–CO wagging |

[a] References 28 and 29. [b] Reference 27.

scribed below. Note the absence of cross contamination of the two samples.

Vibrational frequencies for $CF_3COMn(CO)_5$ are assigned from the comparison with reported results for $CF_3COCl$,[26] $CF_3Mn(CO)_5$,[27] and $C_2F_5COMn(CO)_5$[28] and are listed in Table I. There are four infrared absorption bands for the $CF_3$ group in $CF_3COMn(CO)_5$. The peak at 1254 $cm^{-1}$ is assigned as a symmetric C–F stretch and peaks at 1191 and 1141 $cm^{-1}$ are assigned as an in-plane C–F stretch and an out-of-plane C–F stretch, respectively.[29] The small peak at 719 $cm^{-1}$ is due to a F–$CF_2$ deformation. No vibrational bands fall within the $CO_2$ laser wavelength range (925–1085 $cm^{-1}$).

Infrared absorption bands of (trifluoromethyl)manganese pentacarbonyl have been assigned previously in the literature[27] and are summarized in Table I. The strong peak at 1063 $cm^{-1}$ has been identified as a C–F stretch of $A_1$-type symmetry and the peak at 1043 $cm^{-1}$ as a degenerate C–F stretch of E-type symmetry.[27a] Since the trifluoromethyl ligand exhibits strong absorption bands within the $CO_2$ laser wavelength range, it is an ideal probe ligand to study the infrared multiphoton dissociation processes of organometallic compounds.

The CO stretching vibrations for $CF_3COMn(CO)_5$ are symmetric stretching of equatorial CO at 2134 $cm^{-1}$ ($A_1$-type symmetry), degenerate stretching of equatorial CO at 2050 $cm^{-1}$ (E-type symmetry), symmetric stretching of axial CO at 2028 $cm^{-1}$ ($A_1$-type symmetry), and an acyl CO stretch at 1673 $cm^{-1}$. $CF_3Mn(CO)_5$ shows symmetric and degenerate stretchings of equatorial CO at 2142 ($A_1$) and 2055 (E) $cm^{-1}$, respectively, which are slightly greater than those for $CF_3COMn(CO)_5$ by 8 and 5 $cm^{-1}$, respectively. This result indicates that the $CF_3$ ligand is a poorer $\sigma$ donor than the $CF_3CO$ ligand, leading to less electron density on manganese available for $\pi$ back-donation to the equatorial CO.[30,31] The symmetric stretching vibration for the axial CO in $CF_3Mn(CO)_5$ peaks at 2026 $cm^{-1}$, which is 2 $cm^{-1}$ less than the axial CO stretch in $CF_3COMn(CO)_5$. It has been previously suggested that the force constants of all carbonyl groups in $LMn(CO)_5$ complexes will change by the same amount owing to the change in inductive effect in going from one ligand to another, while the differences in $\pi$ bonding between two ligands will affect the trans force constant twice as much as the cis.[31] This means that the $CF_3CO$ ligand considerably increases an axial CO stretching frequency due to its greater $\pi$-acceptor ability than the $CF_3$ ligand. However, it is evident that both $CF_3$ and $CF_3CO$ ligands are weaker $\pi$-acceptors than CO,[31] because stretching vibrations for axial carbonyls trans to these ligands are much weaker than those for equatorial carbonyls trans to the carbonyls. This result also implies that the Mn–$(CO)_{ax}$ bond is significantly stronger than the Mn–$(CO)_{eq}$ bond. Bond energies of $D[(CO)_5Mn–CF_3]$ = 48.9 kcal/mol and $D[(CO)_5Mn–COCF_3]$ = 42.9 kcal/mol have been reported previously.[6] The $CF_3$ ligand forms a stronger bond than the $CF_3CO$ ligand because the $\sigma$ orbital of trifluoromethyl has considerably more carbon 2s character than that of trifluoroacetyl, resulting in a significant shortening of the Mn–$CF_3$ bond.[32]

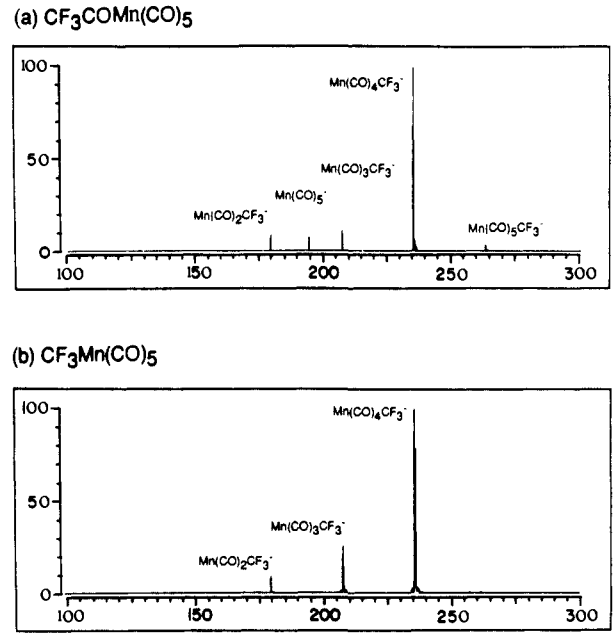


Figure 2. Anion mass spectra of (trifluoroacetyl)manganese pentacarbonyl (a) and (trifluoromethyl)manganese pentacarbonyl (b) with 2-eV electron energy at 4 × $10^{-8}$ Torr.

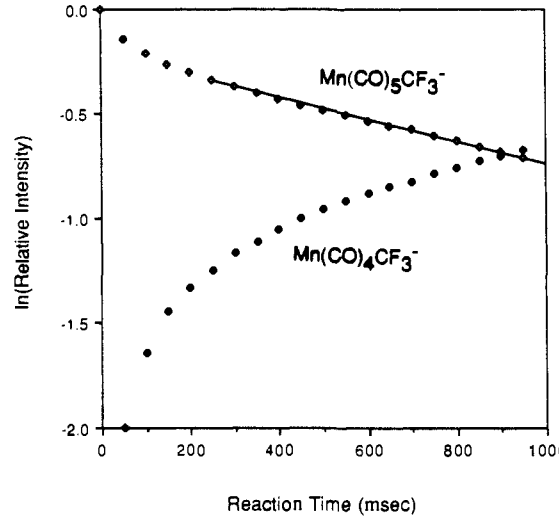


Figure 3. Temporal variation of $Mn(CO)_5CF_3^-$, generated from dissociative electron attachment of (trifluoroacetyl)manganese pentacarbonyl, and its decomposition product $Mn(CO)_4CF_3^-$ at 6.3 × $10^{-8}$ Torr. The limiting slope for the disappearance of the reactant ion yields a rate constant of 2.4 × $10^{-12}$ $cm^3$ $molecule^{-1}$ $s^{-1}$.

**Reactions of $Mn(CO)_nCF_3^-$ Ions.** Dissociative electron attachment by $CF_3COMn(CO)_5$ produces $Mn(CO)_nCF_3^-$ ($n$ = 2–5) and $Mn(CO)_5^-$ fragment ions as shown in Figure 2a. Similarly, $CF_3Mn(CO)_5$ yields $Mn(CO)_nCF_3^-$ ($n$ = 2–4) ions as shown in Figure 2b. $Mn(CO)_5CF_3^-$ and $Mn(CO)_5^-$ ions are characteristic of the $CF_3COMn(CO)_5$ precursor. The latter ion is unreactive with the neutral precursor. $Mn(CO)_5CF_3^-$ derived from $CF_3COMn(CO)_5$ slowly decomposes in thermal collisions with the parent molecule to yield $Mn(CO)_4CF_3^-$ with loss of CO with a rate constant of 2.4 × $10^{-12}$ $cm^3$ $molecule^{-1}$ $s^{-1}$ as shown in Figure 3. The most abundant ions, $Mn(CO)_4CF_3^-$, formed from the two precursors are very stable and unreactive with their neutral

(26) Berney, C. V. *Spectrochim. Acta* **1964**, *20*, 1437.
(27) (a) Colton, F. A.; Wing, R. M. *J. Organomet. Chem.* **1967**, *9*, 511. (b) Cotton, F. A.; Musco, A.; Yagupsky, G. *Inorg. Chem.* **1967**, *6*, 1357.
(28) Pilcher, E.; Stone, F. G. *Spectrochim. Acta* **1962**, *18*, 585.
(29) Ogilvie, J. F. *J. Chem. Soc., Chem. Commun.* **1970**, 323.
(30) Avanzino, S. C.; Bakke, A. A.; Chen, H.-W.; Donahue, C. J.; Jolly, W. L.; Lee, T. H.; Ricco, A. J. *Inorg. Chem.* **1980**, *19*, 1931.
(31) Graham, A. G. *Inorg. Chem.* **1968**, *7*, 315.
(32) Hall, M. B.; Fenske, R. F. *Inorg. Chem.* **1972**, *11*, 768.

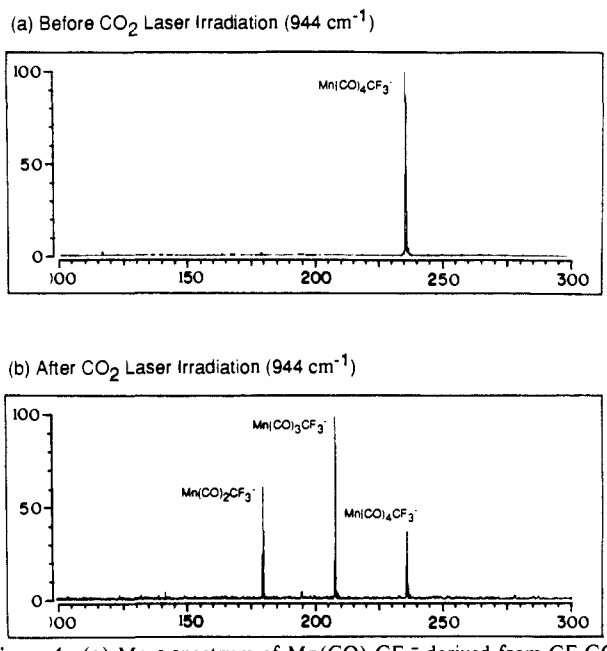


Figure 4. (a) Mass spectrum of $Mn(CO)_4CF_3^-$ derived from $CF_3CO$-$Mn(CO)_5$ 1 ms after a series of ion ejection pulses to remove all other ions except the ion of interest. (b) Photodissociation mass spectrum of $Mn(CO)_4CF_3^-$ at 944 $cm^{-1}$ with an 8 W $cm^{-2}$ laser beam and 20 ms duration. The parent neutral pressure is $2.5 \times 10^{-8}$ Torr.

precursors. $Mn(CO)_3CF_3^-$ generated from the two precursors also slowly decomposes to yield $Mn(CO)_2CF_3^-$ with loss of CO with a rate constant of $4.4 \times 10^{-12}$ $cm^3$ $molecule^{-1}$ $s^{-1}$. $Mn(CO)_2CF_3^-$ ions are unreactive with their neutral partners.

**Infrared Multiphoton Dissociation Spectra of $Mn(CO)_4CF_3^-$ Ions.** $Mn(CO)_4CF_3^-$ ions formed by dissociative electron attachment of two different precursors, (trifluoroacetyl)- or (trifluoromethyl)manganese pentacarbonyl, afford the possibility of observing trifluoroacetyl or trifluoromethyl manganese ions of the same mass-to-charge ratio (VI and VII, respectively).

Figure 4a presents a spectrum of the isolated $Mn(CO)_4CF_3^-$ ion generated from $CF_3COMn(CO)_5$ just after a series of ejection pulses. Figure 4b shows the appearance spectrum of the photodissociation fragments of $Mn(CO)_4CF_3^-$ at 944 $cm^{-1}$ with the 20 ms duration of an 8 W $cm^{-2}$ laser beam. $Mn(CO)_4CF_3^-$ loses CO to yield $Mn(CO)_3CF_3^-$, which undergoes infrared multiphoton dissociation to form $Mn(CO)_2CF_3^-$. The photodissociation spectrum of $Mn(CO)_4CF_3^-$ is obtained by taking the ratio of the parent ion intensity $[Mn(CO)_4CF_3^-]$ to the total ion intensity $[Mn(CO)_4CF_3^- + Mn(CO)_3CF_3^- + Mn(CO)_2CF_3^-]$ as a function of laser wavelength.

Figure 5 shows the infrared absorption spectrum of the $CF_3$ group in $CF_3Mn(CO)_5$ over the $CO_2$ laser wavelength range (a), the infrared multiphoton dissociation spectra of $Mn(CO)_4CF_3^-$ derived from $CF_3COMn(CO)_5$ (b), and $Mn(CO)_4CF_3^-$ obtained from $CF_3Mn(CO)_5$ (c). The infrared photodissociation spectrum of $Mn(CO)_4CF_3^-$ derived from $CF_3COMn(CO)_5$ (Figure 5b) shows broad bands at two maxima at 1052 and 945 $cm^{-1}$ which, within experimental errors, coincides exactly with spectral features in the photodissociation spectrum of the same mass ion generated from $CF_3Mn(CO)_5$ (Figure 5c).

Figure 6 shows the photoproduct appearance spectra of $Mn(CO)_3CF_3^-$ from the infrared multiphoton dissociation of $Mn(CO)_4CF_3^-$. Two spectra from different precursors, $CF_3CO$-$Mn(CO)_5$ (a) and $CF_3Mn(CO)_5$ (b), match well with each other. The further photodissociation of $Mn(CO)_3CF_3^-$ ions during laser irradiation resulted in $Mn(CO)_2CF_3^-$ with loss of CO. The photoproduct spectra of $Mn(CO)_2CF_3^-$ ions in Figure 7 shows similar appearance bands as $Mn(CO)_3CF_3^-$ ions. This indicates that $Mn(CO)_3CF_3^-$ has infrared absorption bands that strongly overlap those of the $Mn(CO)_4CF_3^-$ ion because the appearance spectra of the photoproducts reflect absorption bands of the photodissociating reactants.

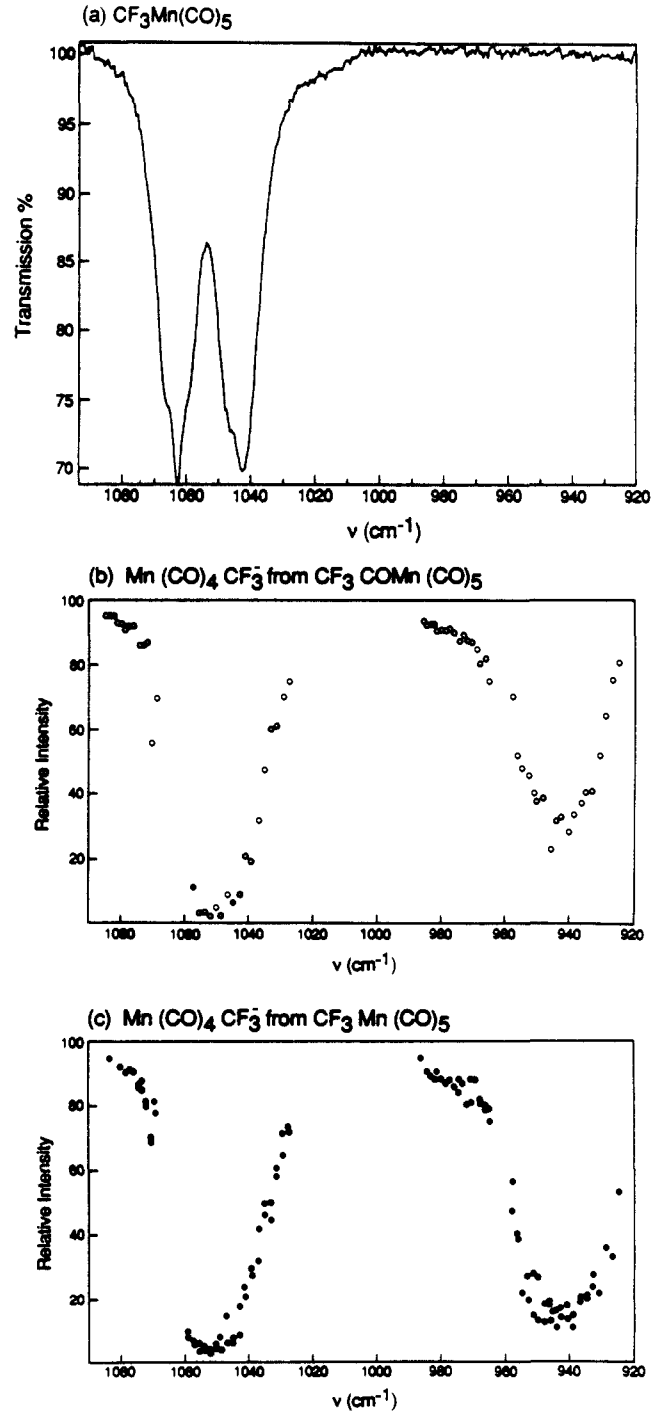


Figure 5. The infrared absorption spectra of the $CF_3$ group in (trifluoromethyl)manganese pentacarbonyl (a) and photodissociation spectra of $Mn(CO)_4CF_3^-$ ions over the $CO_2$ laser spectral range from the two different precursors, (trifluoroacetyl)manganese pentacarbonyl (b) and (trifluoromethyl)manganese pentacarbonyl (c). Parent neutral pressures are $2.5 \times 10^{-8}$ Torr. Data points are the ratio (in percentage) of the intensity of $Mn(CO)_4CF_3^-$ to the total ion intensity $[Mn(CO)_4CF_3^- + Mn(CO)_3CF_3^- + Mn(CO)_2CF_3^-]$ as a function of wavelength. The mass-selected ion of interest is irradiated for 20 ms at 8 W $cm^{-2}$.

**Collision-Induced Dissociation Spectra of $Mn(CO)_4CF_3^-$ Ions.** Figure 8 shows the collision-induced dissociation spectra of $Mn(CO)_4CF_3^-$ ions from $CF_3COMn(CO)_5$ (a) and $CF_3Mn(CO)_5$ (b) precursors. If the $Mn(CO)_4CF_3^-$ ion derived from $CF_3CO$-$Mn(CO)_5$ contains the trifluoroacetyl group, then the $Mn(CO)_3^-$ ion would be present in the collision-induced dissociation spectrum by loss of $CF_3CO$. Collisions of $Mn(CO)_4CF_3^-$ ions from two different precursors with Ar or Kr buffer gas induce identical dissociation patterns without any indication of $Mn(CO)_3^-$ fragment

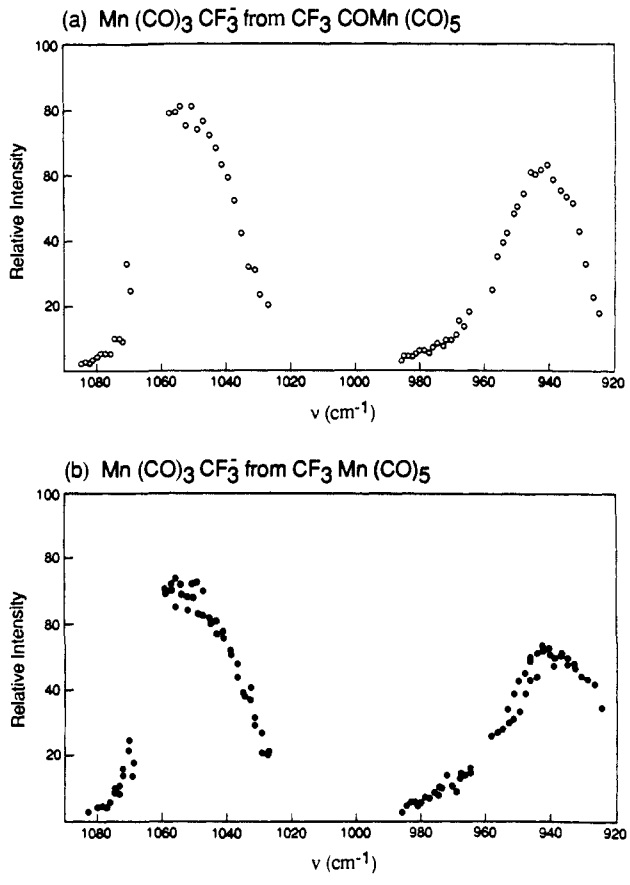


Figure 6. Photoappearance spectra of $Mn(CO)_3CF_3^-$ ions over the $CO_2$ laser spectral range from the two different precursors, (trifluoroacetyl)manganese pentacarbonyl (a) and (trifluoromethyl)manganese pentacarbonyl (b). Data points are the ratio (in percentage) of the intensiiy of $Mn(CO)_3CF_3^-$ to the total ion intensity [$(Mn(CO)_4CF_3^-$ + $Mn(CO)_3CF_3^-$ + $Mn(CO)_2CF_3^-$] as a function of wavelength.

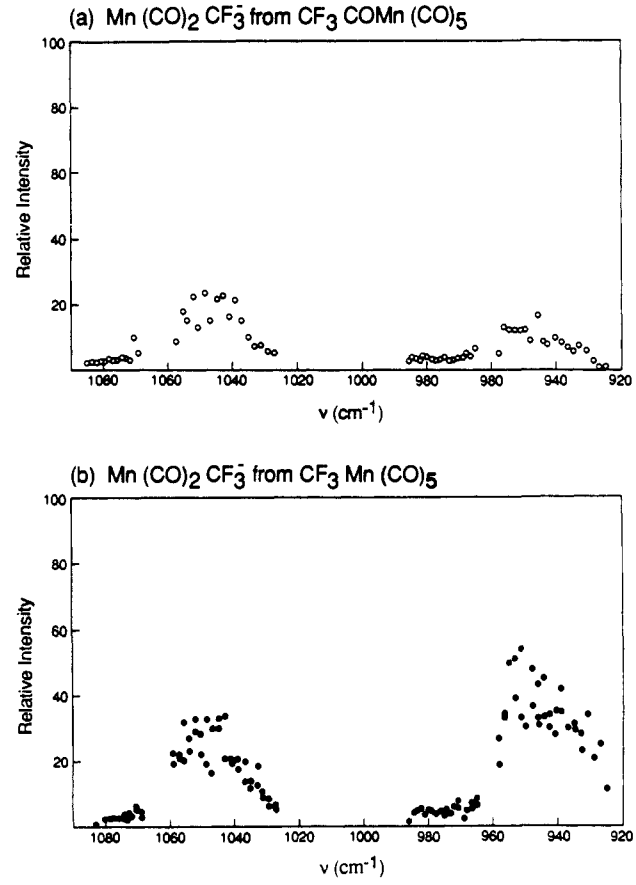


Figure 7. Photoappearance spectra of $Mn(CO)_2CF_3^-$ ions over the $CO_2$ laser spectral range from the two different precursors, (trifluoroacetyl)manganese pentacarbonyl (a) and (trifluoromethyl)manganese pentacarbonyl (b). Data points are the ratio (in percentage) of the intensity of $Mn(CO)_2CF_3^-$ to the total ion intensity [$Mn(CO)_4CF_3^-$ + $Mn(CO)_3CF_3^-$ + $Mn(CO)_2CF_3^-$] as a function of wavelength.

ions expected from the $CF_3COMn(CO)_3^-$ ion if present. The translational energy imparted to an ion is estimated to be about 84 eV (corresponding to center of mass collision energies of 12 and 22 eV, respectively, for Ar and Kr). $MnCF_3^-$ is the most intense fragment ion observed after collision-induced dissociation. The intensity of the $Mn(CO)_3CF_3^-$ ion is very weak compared with the infrared multiphoton dissociation process, which manifests that the collision-induced dissociation is a higher energy activation process than the infrared multiphoton dissociation which proceeds selectively by the pathway with the lowest activation energy.[18,33]

**Ligand-Displacement Reactivities of $Mn(CO)_4CF_3^-$ Ions.** We have examined ligand displacement reactions of $Mn(CO)_4CF_3^-$ ions from the two precursors with the strong $\pi$-acids,[34] $^{13}CO$, $PF_3$, and NO. If $Mn(CO)_4CF_3^-$ generated from $CF_3COMn(CO)_5$ is $CF_3COMn(CO)_3^-$, the reactivity of ligand displacement of this 15 $e^-$ anion with the strong $\pi$-acids might be quite different from that of the 17 $e^-$ $CF_3Mn(CO)_4^-$ ion.

The thermoneutral ligand displacement reaction of $Mn(CO)_4CF_3^-$ ions with $^{13}CO$ does not occur. No ligand displacement is observed in the reaction of $Mn(CO)_4CF_3^-$ ions with the stronger $\pi$-acceptor $PF_3$.[34] Corderman and Beauchamp[35] have observed the ligand displacement reaction of the 17 $e^-$ $\eta^5$-CpCo(CO)$^-$ (cyclopentadienylcobalt carbonyl) ion with $PF_3$ to yield the 17 $e^-$ $\eta^5$-$CpCoPF_3^-$ ion with loss of CO, presumably via ring slippage forming the 15 $e^-$ $\eta^3$-CpCo(CO)$^-$ intermediate. In light of these results, it is reasonable to suggest that $Mn(CO)_4CF_3^-$ is the 17 $e^-$ complex and does not undergo the $CF_3$ migration forming the 15 $e^-$ $CF_3COMn(CO)_3^-$ intermediate during the thermal bimolecular encounter.

(a) CID spectrum of $Mn(CO)_4CF_3^-$ from $CF_3COMn(CO)_5$ with Ar

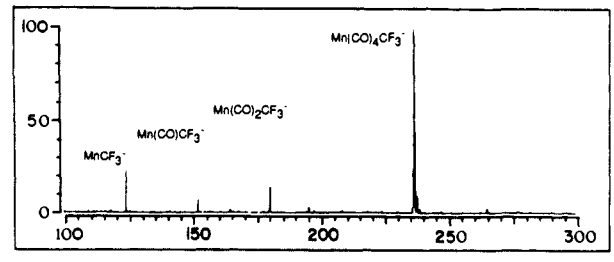


(b) CID spectrum of $Mn(CO)_4CF_3^-$ from $CF_3Mn(CO)_5$ with Ar

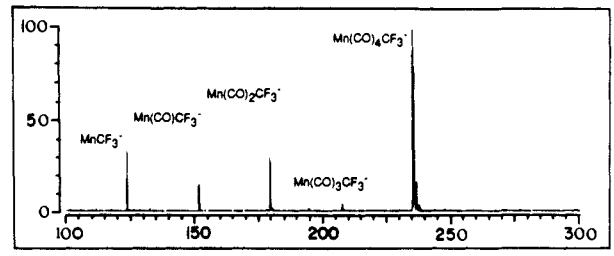


Figure 8. The collision-induced dissociation spectra of $Mn(CO)_4CF_3^-$ ions from the two different precursors, (trifluoroacetyl)manganese pentacarbonyl (a) and (trifluoromethyl)manganese pentacarbonyl (b) with Ar buffer gas; $P$(the parent neutral) = $4 \times 10^{-8}$ Torr, $P$(Ar) = $4 \times 10^{-6}$ Torr, and $E_{CM}$(collision) = 12 eV.

(33) Watson, C. H.; Baykut, G.; Battiste, M. A.; Eyler, J. R. *Anal. Chim. Acta* **1985**, *178*, 125.

(34) (a) Cotton, F. A.; Wilkinson, G. *Advanced Inorganic Chemistry*, 4th ed.; Wiley: New York; 1980. (b) Avanzino, S. C.; Chen, H.-W.; Donahue, C. J.; Jolly, W. L. *Inorg. Chem.* **1980**, *19*, 2201.

(35) Corderman, R. R.; Beauchamp, J. L. *Inorg. Chem.* **1977**, *16*, 3135.

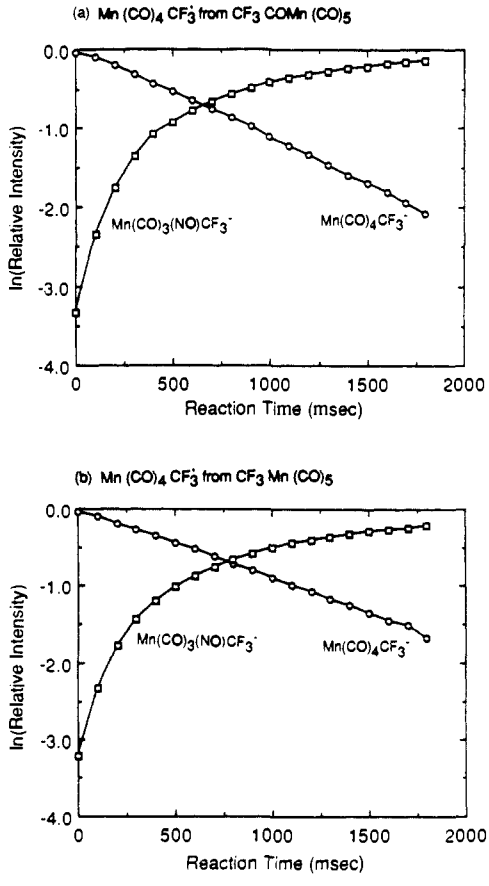


Figure 9. Temporal variation of $Mn(CO)_4CF_3^-$ ions, generated from the two different precursors, (trifluoroacetyl)manganese pentacarbonyl (a) and (trifluoromethyl)manganese pentacarbonyl (b), and $Mn(CO)_3(NO)CF_3^-$ in the ligand displacement reaction: (a) $P[CF_3COMn(CO)_5] = 4.1 \times 10^{-8}$ Torr and $P(NO) = 6.7 \times 10^{-6}$ Torr; (b) $P[CF_3Mn(CO)_5] = 4 \times 10^{-8}$ Torr and $P(NO) = 6 \times 10^{-6}$ Torr.

However, nitric oxide, NO, which can be considered as either 1 $e^-$ or 3 $e^-$ donor, reacts with $Mn(CO)_4CF_3^-$ ions to yield a nitrosyl-containing complex $Mn(CO)_3(NO)CF_3^-$ with loss of one CO (eq 2). $Mn(CO)_4CF_3^-$ ion derived from the $CF_3COMn(CO)_5$

$$Mn(CO)_4CF_3^- + NO \rightarrow Mn(CO)_3(NO)CF_3^- + CO \quad (2)$$

precursor undergoes reaction 2 as shown in Figure 9a with a rate constant of $3.7 \pm 0.7 \times 10^{-12}$ cm$^3$ molecule$^{-1}$ s$^{-1}$, which is in good agreement with the observed rate constant of $4.2 \pm 0.8 \times 10^{-12}$ cm$^3$ molecule$^{-1}$ s$^{-1}$ for the ligand displacement reaction of $Mn(CO)_4CF_3^-$ ion obtained from the $CF_3Mn(CO)_5$ precursor with NO as shown in Figure 9b.

*In light of the similar infrared multiphoton dissociation spectra, the indistinguishable collision-induced dissociation patterns, and the identical rate constants within experimental errors for the ligand displacement reaction with NO, it is quite reasonable to conclude that $Mn(CO)_4CF_3^-$ ions generated from the dissociative electron attachment of two different precursors, $CF_3COMn(CO)_5$ and $CF_3Mn(CO)_5$, are the same 17 $e^-$ species having the trifluoromethyl group directly bonded to the manganese, which is a (trifluoromethyl)manganese tetracarbonyl ion (VII), $CF_3Mn(CO)_4^-$.*

**Infrared Multiphoton Dissociation of $CF_3COMn(CO)_4^-$ and Mechanism of the Migratory Decarbonylation Reaction.** $Mn(CO)_5CF_3^-$ and its decomposition product $Mn(CO)_4CF_3^-$, which are trapped in the ICR cell after 1-s delay from the initial isolation of $Mn(CO)_5CF_3^-$, are irradiated with an 8 W cm$^{-2}$ $CO_2$ laser beam for 10 ms. Figure 10 shows the mass spectra before (a) and after (b) $CO_2$ laser irradiation at 944 cm$^{-1}$. The absolute intensity of $Mn(CO)_5CF_3^-$ remains constant, while $Mn(CO)_4CF_3^-$ dissociates first to $Mn(CO)_3CF_3^-$ and subsequently yields $Mn(CO)_2CF_3^-$. $Mn(CO)_5CF_3^-$ does not undergo infrared multiphoton dissociation in the 925–1085 cm$^{-1}$ wavelength range. Since the $CF_3CO$ group

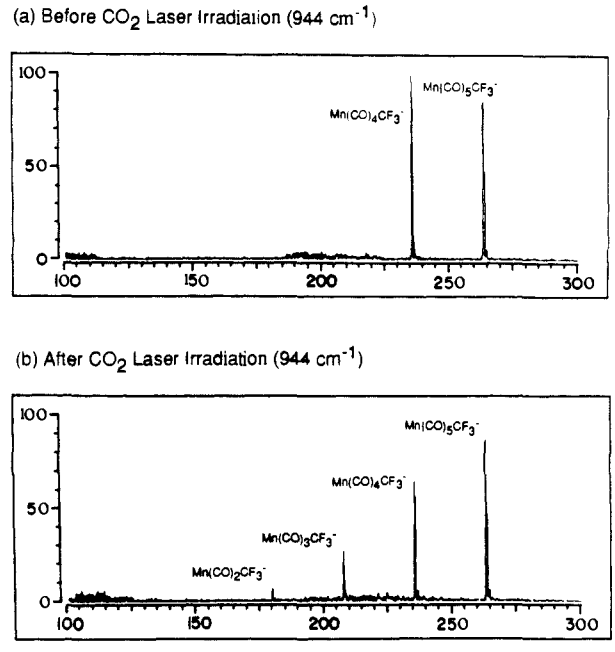


Figure 10. (a) Mass spectrum of $Mn(CO)_5CF_3^-$ derived from $CF_3CO$-$Mn(CO)_5$ and its decomposition product $Mn(CO)_4CF_3^-$ after 1-s delay from the initial isolation of $Mn(CO)_5CF_3^-$. (b) Photodissociation mass spectrum of $Mn(CO)_5CF_3^-$ and $Mn(CO)_4CF_3^-$ at 944 cm$^{-1}$ with an 8 W cm$^{-2}$ laser beam and 10-ms duration. The parent neutral pressure is $5 \times 10^{-8}$ Torr.

**Scheme I**

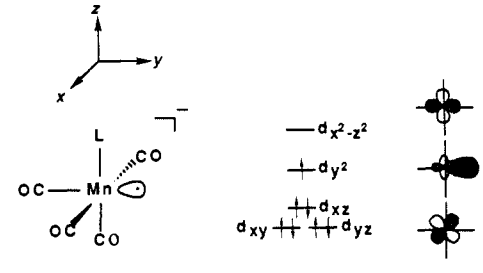


bonded to manganese has no infrared absorption bands in the $CO_2$ laser wavelength range and the decomposition product $Mn(CO)_4CF_3^-$ is proven as $CF_3Mn(CO)_4^-$, $Mn(CO)_5CF_3^-$ ion generated from $CF_3COMn(CO)_5$ is clearly a (trifluoroacetyl)manganese tetracarbonyl anion, $CF_3COMn(CO)_4^-$.

Since the decomposition of $CF_3COMn(CO)_4^-$ yields $CF_3Mn(CO)_4^-$ with loss of CO, it is necessary to invoke the migration of the $CF_3$ group from the acyl carbon to the manganese during the dissociation process. This implies that $CF_3COMn(CO)_4^-$ has a vacant site for the $CF_3$ migration. The structures of the $d^7$ complexes, $CF_3COMn(CO)_4^-$ and $CF_3Mn(CO)_4^-$, are presumed to be square-based pyramid with $CF_3CO$ and $CF_3$ in the basal planes, respectively, from comparisons with results for other $d^6$ and $d^7$ five-coordinate manganese complexes. An infrared spectroscopic study of the five-coordinate $d^6$ complex, $CH_3CO$-$Mn(CO)_4$, in methane matrix at 12 K indicates the square-based pyramidal structure with $\eta^1$-acyl bonding.[36] Spectroscopic studies of the $d^7$ complex, $Mn(CO)_5$, generated in $Cr(CO)_6$ crystals or in low-temperature solid matrices, support a square-pyramidal structure with $C_{4v}$ point group.[37] Extended Hückel calculations

(36) Hitam, R. B.; Narayanaswamy, R.; Resi, A. J. *J. Chem. Soc., Dalton Trans.* **1983**, 615.

(37) (a) Hughey, J. L.; Anderson, C. P.; Meyer, T. J. *J. Organomet. Chem.* **1977**, *125*, C49. (b) Waliz, W. L.; Hackelberg, O.; Dorfman, L. M.; Wojcicki, A. *J. Am. Chem. Soc.* **1978**, *100*, 7259. (c) Church, S. P.; Poliakoff, M.; Timney, J. A.; Turner, J. J. *J. Am. Chem. Soc.* **1981**, *103*, 7515. (d) Symons, M. C. R.; Sweany, R. L. *Organometallics* **1982**, *1*, 834. (e) Fairhursi, S. A.; Morion, J. R.; Perutz, R. N.; Presion, K. F. *Organometallics* **1984**, *3*, 1389. (f) Howard, J. A.; Morion, J. R.; Presion, K. F. *Chem. Phys. Lett.* **1981**, *83*, 226. (g) Lionel, T.; Morion, J. R.; Preston, K. F. *Chem. Phys. Lett.* **1981**, *81*, 17.

Scheme II

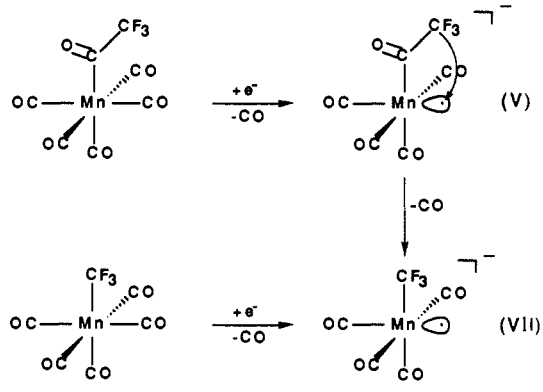


by Elian and Hoffmann[38] also suggest the square-pyramidal structure for the five-coordinate $d^7$ complex carrying its odd electron in a relatively high-lying, directional orbital of $A_1$ symmetry. Low-lying occupied d orbitals for the $d^7$ square-pyramidal $LMn(CO)_4^-$ (L = $CF_3CO$, $CF_3$) are shown in Scheme I.

The present experimental result combined with the presumed square-pyramidal structures for ions of interest elucidates the stepwise dissociative electron attachment process in the generation of $CF_3Mn(CO)_4^-$ from the $CF_3COMn(CO)_5$ precursor as shown in Scheme II. Since the $Mn-(CO)_{eq}$ bond is weaker than the $Mn-(CO)_{ax}$ bond and the decomposition of $CF_3COMn(CO)_4^-$ ion necessitates the migration of the $CF_3$ group to an empty apical site, the generation of $CF_3Mn(CO)_4^-$ from the $CF_3COMn(CO)_5$ precursor involves an electron attachment with loss of an equatorial CO forming $CF_3COMn(CO)_4^-$ (V) followed by the migration of the $CF_3$ group from the acyl carbon to the apical position with loss of the second carbonyl cis to $CF_3$. It will be of particular experimental interest to see whether this $CF_3$ migratory decarbonylation occurs via a stepwise or concerted mechanism. The acyl oxygen-18 labeled $CF_3C^{18}OMn(CO)_5$ precursor would produce $CF_3C^{18}OMn(CO)_4^-$ by dissociative electron attachment, and its subsequent decomposition would yield the unlabeled $CF_3Mn(CO)_4^-$ by the concerted loss of acyl $C^{18}O$ or both the oxygen-18 labeled and unlabeled products by the stepwise loss of CO.

The production of $CF_3Mn(CO)_4^-$ from the $CF_3Mn(CO)_5$ precursor is presumably via the electron attachment with loss of an equatorial CO, because the $\pi$ back-bonding with an axial CO is significantly stronger than that with an equatorial CO [$\nu_s(CO_{ax})$ = 2026 $cm^{-1}$ and $\nu_s(CO_{eq})$ = 2142 $cm^{-1}$] and the difference in $CF_3Mn(CO)_5$ [$\Delta\nu_s(CO)$ = 116 $cm^{-1}$] is even greater than that in $CF_3COMn(CO)_5$ [$\Delta\nu_s(CO)$ = 106 $cm^{-1}$]. This likely results in a square-pyramidal structure (VII) for $CF_3Mn(CO)_4^-$.

**Kinetics and Energetics of the Migratory Decarbonylation Reaction.** The kinetics of decomposition of $CF_3COMn(CO)_4^-$ yielding $CF_3Mn(CO)_4^-$ with loss of CO has been examined by adding argon buffer gas and changing the pressures of the parent neutral molecule, $CF_3COMn(CO)_5$, and the buffer gas, Ar. The temporal variations of reactant and product ion abundances at different pressures of the argon buffer gas are shown in Figure 11a and reveal a biexponential decay, which can be deconvoluted to yield the Ar pressure dependent initial fast decay as illustrated in Figure 11b and the Ar pressure independent slow decay as presented in Figure 11c. The slope of the initial fast decay shown in Figure 11b changes from 2.2 $s^{-1}$ at the parent neutral pressure of $2.5 \times 10^{-8}$ Torr to 3.5 $s^{-1}$ by adding $1.1 \times 10^{-6}$ Torr Ar. On the contrary, the slope of the slow decay (Figure 11c) remains constant within experimental error with the addition of the argon buffer gas (from 0.19 $s^{-1}$ at $P[CF_3COMn(CO)_5] = 2.5 \times 10^{-8}$ Torr to 0.20 and 0.19 $s^{-1}$ with the addition of $P(Ar) = 5.5 \times 10^{-7}$ and $1.1 \times 10^{-6}$ Torr, respectively). However, this slow decay slope varies with the parent neutral pressure from 0.19 $s^{-1}$ at $P[CF_3COMn(CO)_5] = 2.5 \times 10^{-8}$ Torr (Figure 11c) to 0.52 $s^{-1}$ at $P[CF_3COMn(CO)_5] = 6.3 \times 10^{-8}$ Torr (Figure 3). This result

(38) Elian, M.; Hoffmann, R. *Inorg. Chem.* **1975**, *14*, 1058.

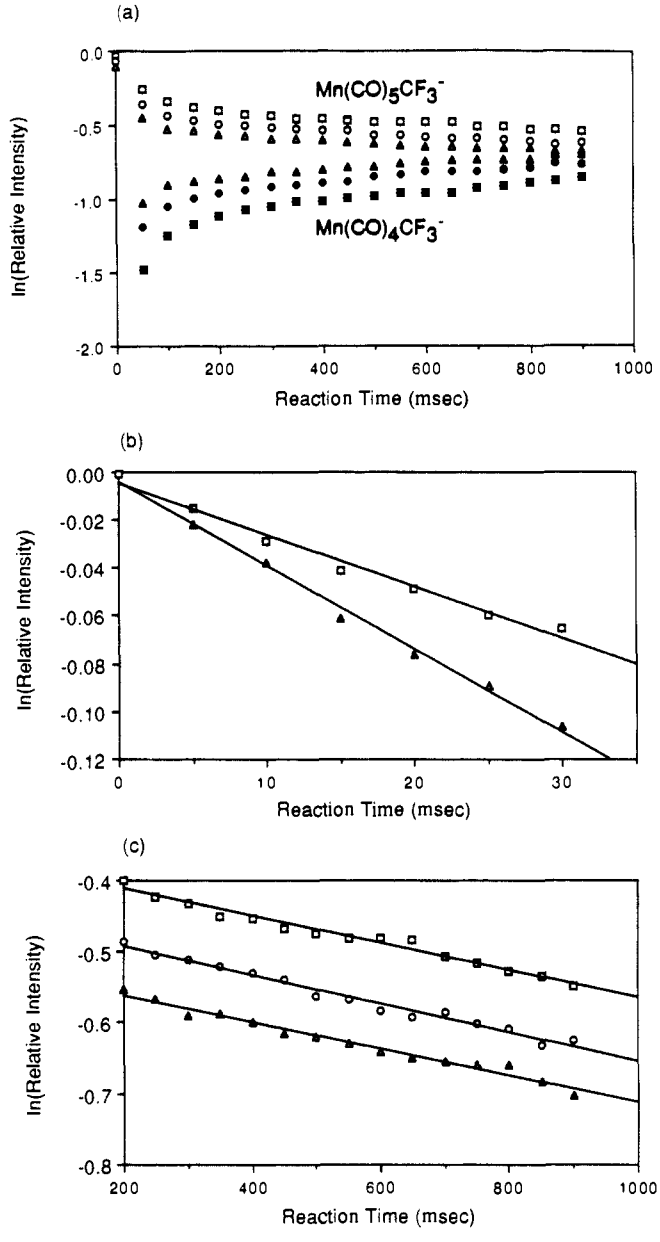


**Figure 11.** (a) Temporal variation of $CF_3COMn(CO)_4^-$ (open) and $CF_3Mn(CO)_4^-$ (solid) at $P[CF_3COMn(CO)_5] = 2.5 \times 10^{-8}$ Torr (square) and with the addition of $P(Ar) = 5.5 \times 10^{-7}$ Torr (circle) and $P(Ar) = 1.1 \times 10^{-6}$ Torr (triangle). (b) The initial Ar pressure dependent fast decay of $CF_3COMn(CO)_4^-$ at $P[CF_3COMn(CO)_5] = 2.5 \times 10^{-8}$ Torr (open square; slope = $-2.2$ $s^{-1}$) and with addition of $P(Ar) = 1.1 \times 10^{-6}$ Torr (open triangle; slope = $-3.5$ $s^{-1}$). (c) The Ar pressure independent slow decay of $CF_3COMn(CO)_5$ at $P[CF_3COMn(CO)_5] = 2.5 \times 10^{-8}$ Torr (open square; slope = $-0.19$ $s^{-1}$) and with the addition of $P(Ar) = 5.5 \times 10^{-7}$ Torr (open circle; slope = $-0.20$ $s^{-1}$) and $P(Ar) = 1.1 \times 10^{-6}$ Torr (open triangle; slope = $-0.19$ $s^{-1}$).

indicates that the decomposition of $CF_3COMn(CO)_4^-$ is a bimolecular process involving the neutral molecule as a collision partner.

Electron impact initially generates vibrationally excited ions with a broad internal energy distribution. The initial fast decay reflects the decomposition of hot ions with energies near the activation barrier and depends upon interaction with a neutral collision partner. However, there is always a competition between decomposition and collisional deactivation of the hot ion. The data in Figure 11 suggest that both argon and $CF_3COMn(CO)_5$ are effective at leading to decomposition of the vibrationally hot ions. In view of the fact that the fraction of stabilized ions decreases with increasing Ar pressure, it is suggested that Ar more effectively leads to decomposition rather than deactivation (in comparison to $CF_3COMn(CO)_5$). This is not surprising because

Scheme III

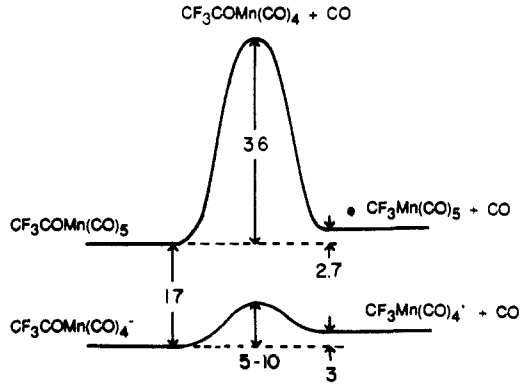


of the possibility of near resonant V–V energy transfer to the polyatomic collision partner. After the collisional deactivation of the hot ion, the decomposition rate is no longer dependent upon the Ar pressure but dependent upon the parent neutral pressure. This specific pressure dependence of the slow decomposition process may provide additional information about the rearrangement and decomposition energetics of $CF_3COMn(CO)_4^-$. Since the driving force of the ion–molecule reaction is primarily the ion-induced dipole interaction, it is reasonable to suggest that the ion–Ar interaction is too weak to induce the migration reaction, whereas, the ion–$CF_3COMn(CO)_5$ interaction is strong enough to drive the migration reaction by lowering the barrier. Therefore, the energy barrier for the migration reaction would be greater than the ion–Ar interaction but less than the ion–$CF_3COMn(CO)_5$ interaction. This provides a rough estimate of the reaction barrier as being in the energy range 5–10 kcal/mol.

Scheme III illustrates potential energy surfaces that emphasize the differences between reactions 3 and 4. Electron affinities of 2.4 eV for five-coordinated complexes, $CF_3COMn(CO)_4$ and $CF_3Mn(CO)_4$, are assumed to be equal to that of $Mn(CO)_5$, which is estimated from the gas-phase acidity of 318 ± 3 kcal/mol for $HMn(CO)_5$[39] combined with $D[(CO)_5Mn–H]$ = 59 kcal/mol[40] and IP(H) = 13.598 eV.

$$CF_3COMn(CO)_5 \rightleftharpoons CF_3COMn(CO)_4 + CO \rightarrow CF_3Mn(CO)_5 + CO \quad (3)$$

$$CF_3COMn(CO)_4^- \rightarrow CF_3Mn(CO)_4^- + CO \quad (4)$$

Since reaction 3 involves a rate-determining decarbonylation step[2] followed by the methyl migration, an activation energy as high as the Mn–CO bond dissociation energy would be required. Providing that $D[CF_3COMn(CO)_4–CO]$ is equal to $D[Mn_2(CO)_9–CO]$ = 36 ± 2 kcal/mol[41] leads to an activation barrier estimate of 36 kcal/mol for reaction 3. Note that with these estimates for $EA[CF_3COMn(CO)_4]$ and $D[CF_3COMn(CO)_4–CO]$ the initial electron-attachment process with loss of a first CO (upper step in Scheme II) is exothermic by at least 17 kcal/mol as illustrated in Scheme III. If the slow migratory decarbonylation rate of reaction 4 is due to a barrier, the proposed barrier height of 5–10 kcal/mol is significantly smaller than that of reaction 3. In view of the low barrier proposed for further decarbonylation, it is not surprising that the majority of the attaching species lose a second CO (Figure 2a) and a vibrationally hot population is prevalent. The small activation barrier for reaction 4 also suggests that the $CF_3$ migration occurs either prior to or in concert with decarbonylation, which would otherwise require a high activation barrier as a first step. However, it is yet to be explored whether the decarbonylation undergoes a stepwise mechanism involving a transient 19 $e^-$ intermediate or a concerted mechanism involving exclusive loss of acyl carbonyl.

The enthalpy change for the migratory decarbonylation reaction 3 is estimated to be 2.7 ± 1.7 kcal/mol from the gas phase heats of formation of $CF_3COMn(CO)_5$, $CF_3Mn(CO)_5$, and CO.[42] The overall decomposition reaction 4 is probably endothermic by about 3 kcal/mol. However, the free energy change for the migratory decarbonylation reaction is expected to be quite negative due to loss of free CO. Since the translational and rotational contribution to the entropy of CO is about 47.4 cal $mol^{-1}$ $K^{-1}$,[43] the overall entropy change for the process is probably not less than this CO entropy increase. The estimated free energy change for reaction 4 at 298 K is about −12 kcal/mol.

Table II. The C–F Stretching Frequencies of $CF_3X$ Molecules[a]

| molecule | $\nu_3(a_1)$, $cm^{-1}$ | $\nu_3$(e or f), $cm^{-1}$ |
|---|---|---|
| $CF_3$ | 1084 | 1250 |
| $CF_3H$ | 1137 | 1157 |
| $CF_3D$ | 1111 | 1210 |
| $CF_3I$ | 1076 | 1183 |
| $CF_3Br$ | 1087 | 1206 |
| $CF_3Cl$ | 1102 | 1210 |
| $CF_3F$ | 904 | 1265 |
| $CF_3CH_3$ | 1278 | 1230 |
| $CF_3CCl_3$ | 1255 | 1227 |
| $CF_3CF_3$ | 1417, 1117 (1267)[b] | 1250, 1250.5 (1250)[b] |
| $CF_3C{\equiv}CCF_3$ | 1245, 1294 (1270)[b] | 1181, 1198 (1190)[b] |
| $CF_3C{\equiv}CH$ | 1254 | 1182 |
| $CF_3C{\equiv}N$ | 1221 | 1212 |
| $CF_3Mn(CO)_5$[c] | 1063 | 1043 |
| $CF_3Mn(CO)_4^-$[d] | 1052 | 945 |

[a] From ref 26. [b] Mean value. [c] Reference 2 and this work. [d] This work.

Scheme IV

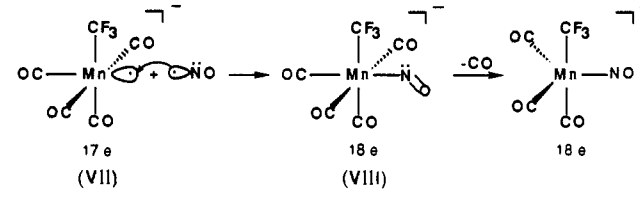


**Vibrational Frequency Assignments.** The assignments of the observed C–F stretching frequencies in the infrared multiphoton dissociation spectra of $CF_3Mn(CO)_4^-$ are made by comparison with results for other $CF_3X$ molecules[27,28] summarized in Table II. It has been noticed previously that the nondegenerate C–F stretching mode is higher in frequency than the degenerate C–F stretching mode, where the $CF_3$ group is attached to a carbon atom in a molecule of $C_{3v}$ symmetry.[27] This holds for molecules of $D_{3d}$ symmetry (e.g. $CF_3CF_3$ and $CF_3C{\equiv}CCF_3$) if the mean of the two nondegenerate stretching vibrations ($A_{1g}$ and $A_{1u}$) is compared with the mean of the two degenerate vibrations ($E_g$ and $E_u$). If the $CF_3$ group is attached to a hydrogen or halogen atom, the degenerate stretch is the higher. Cotton and Wing[27] have also concluded that the nondegenerate C–F stretching frequency in $CF_3Mn(CO)_5$ is higher than the degenerate C–F stretching mode. Assuming the higher frequency for the nondegenerate C–F stretching mode leads to the assignments of 1052 $cm^{-1}$ as a symmetric C–F stretch of $A_1$-type symmetry and 945 $cm^{-1}$ as a degenerate C–F stretch of E-type symmetry. It is quite surprising

(39) Stevens, A. E. Ph.D. Thesis, California Institute of Technology, Pasadena, 1981.

(40) Heats of formation of −177 ± 2 kcal/mol for $HMn(CO)_5$ and −379 ± 1 kcal/mol for $Mn_2(CO)_{10}$ (ref 42), combined with $D[(CO)_5Mn–Mn(CO)_5]$ = 38 ± 5 kcal/mol and $\Delta H_f°_{298}(H)$ = 52.1 kcal/mol, lead to $D[(CO)_5Mn–H]$ = 59 ± 6 kcal/mol. The value for D(Mn–Mn) is taken from recent photoacoustic calorimetry studies (Goodman, J. L.; Peters, K. S.; Vaida, V. *Organometallics* **1986**, *6*, 815), which is in agreement with a value of 41 ± 9 kcal/mol obtained from ion cyclotron resonance and photoelectron studies (Simões, J. A. M.; Schultz, J. C.; Beauchamp, J. L. *Organometallics* **1985**, *4*, 1238).

(41) See ref 1b, p 240.

(42) Connor, J. A.; Zafarani-Moattar, M. T.; Bickerton, J.; El Saied, N. I.; Suradi, S.; Carson, R.; Al Takhin, G.; Skinner, H. A. *Organometallics* **1982**, *1*, 1166.

(43) Calculated from formulae in *JANAF Thermochemical Tables*, 2nd ed.; Stull, D. R., Prophet, H., Eds.; NBS: Washington, DC, 1971.

to observe that the symmetric C-F stretching mode has changed very little in frequency from 1063 $cm^{-1}$ for $CF_3Mn(CO)_5$ to 1052 $cm^{-1}$ for $CF_3Mn(CO)_4^-$, whereas the frequency of the degenerate C-F stretching mode of E-type symmetry has decreased from 1043 $cm^{-1}$ for $CF_3Mn(CO)_5$ to 945 $cm^{-1}$ for $CF_3Mn(CO)_4^-$.

**Ligand Displacement Reaction Mechanism.** The square-based pyramidal $CF_3Mn(CO)_4^-$ ion reacts with NO to produce $CF_3Mn(CO)_3(NO)^-$ with loss of CO. The proposed association mechanism for the ligand displacement reaction is shown in Scheme IV.

It is suggested that the reaction of NO with the 17 $e^-$ $CF_3Mn(CO)_4^-$ ion (VII) involves an approach of NO to a singly occupied orbital on the apical site to form an 18 $e^-$ intermediate (VIII) having a bent Mn-NO bond (1 $e^-$ donor) followed by loss of equatorial carbonyl trans to NO, with charge transfer from nitrogen to metal forming a linear Mn-N-O bond (3 $e^-$ donor). It has been previously shown that several metal nitrosyl carbonyl compounds (e.g. $V(CO)_5(NO)$, $Mn(CO)_4(NO)$, and $Co(CO)_3(NO)$) undergo ligand displacement reactions via an associative ($SN_2$) pathway involving a bent metal nitrosyl intermediate.[44] Lionel et al.[45] have observed the electron paramagnetic resonance spectrum of $Mn(CO)_4(NO)^-$ doped in $Cr(CO)_6$ single crystals suggesting that the Mn-N-O moiety is bent. These observations support the proposed associative mechanism for the ligand displacement reaction. The resulting ion is formally an 18 $e^-$ complex and presumed to have a trigonal-bipyramidal structure with a linear Mn-NO in the equatorial position.[46] Frenz et al.[47] have determined the crystal structure of $Mn(CO)_4(NO)$, revealing that the nitrosyl group is in an equatorial position in the trigonal-bipyramidal structure and the Mn-CO and Mn-NO bonds are linear. $Mn(CO)_5^-$ also has a trigonal-bipyramidal structure in the solid state.[48]

## Conclusion

The $CF_3$ migratory decarbonylation reaction of $CF_3COMn(CO)_4^-$ yielding $CF_3Mn(CO)_4^-$ with loss of CO is observed in the gas phase. The structures of the reactant and product ions are elucidated by employing various mass spectrometric techniques. The kinetic studies of decomposition of $CF_3COMn(CO)_4^-$ show that the $CF_3$ migration occurs with a small barrier either prior to or in concert with decarbonylation.

The $CF_3$ group bonded to a transition-metal center is an ideal infrared chromophore to investigate the infrared photochemistry of organometallic complexes. These studies yield information related to the structure and reaction mechanisms of coordinatively unsaturated organometallic intermediates. It will be of further experimental and theoretical interest to see how the C-F stretching frequencies vary with the number and variety of ligand substituents in complexes containing metal-bonded $CF_3$ groups.

**Acknowledgment.** S.K.S. acknowledges the assistance of J. W. Park for the synthesis and J. E. Hanson for the FT-IR spectra. We also acknowledge the support of the National Science Foundation (Grant No. CHE87-11567) and the donors of the Petroleum Research Fund, administered by the American Chemical Society.

(44) Basolo, F. *Inorg. Chim. Acta* **1985**, *33*, 100.
(45) Lionel, T.; Morton, J. R.; Preston, K. F. *J. Phys. Chem.* **1982**, *86*, 367.
(46) Shin, S. K.; Beauchamp, J. L. *J. Am. Chem. Soc.* submitted for publication.
(47) Frenz, B. A.; Enemark, J. H.; Ibers, J. A. *Inorg. Chem.* **1969**, *8*, 1288.
(48) Frenz, B. A.; Ibers, J. A. *Inorg. Chem.* **1972**, *11*, 1109.

# Infrared Multiphoton Dissociation Spectrum of $CF_3Mn(CO)_3(NO)^-$

**Seung Koo Shin and J. L. Beauchamp***

*Contribution No. 7952 from the Arthur Amos Noyes Laboratory of Chemical Physics, California Institute of Technology, Pasadena, California 91125.* *Received August 9, 1989*

**Abstract:** An infrared multiphoton dissociation spectrum of $CF_3Mn(CO)_3(NO)^-$ has been obtained with Fourier transform ion cyclotron resonance spectroscopy combined with a line-tunable continuous wave $CO_2$ laser in the 925-1085 $cm^{-1}$ wavelength range. The trifluoromethyl group in the anion shows two absorption maxima at 1045 and 980 $cm^{-1}$. The peak at 1045 is assigned as a C-F stretch of $A_1$-type symmetry and the peak at 980 $cm^{-1}$ is ascribed to a C-F stretch of E-type symmetry. It is quite interesting to observe that the symmetric C-F stretching mode changes little in frequency from 1063 $cm^{-1}$ for $CF_3Mn(CO)_5$ to 1045 $cm^{-1}$ for $CF_3Mn(CO)_3(NO)^-$, while the C-F stretching frequency of E-type symmetry decreases from 1043 $cm^{-1}$ for the 18 $e^-$ neutral precursor to 980 $cm^{-1}$ for the 18 $e^-$ anion. Comparison with the infrared multiphoton dissociation spectrum of $CF_3Mn(CO)_4^-$ ion reveals that the degenerate C-F stretch of E-type symmetry increases from 945 $cm^{-1}$ for the 17 $e^-$ $CF_3Mn(CO)_4^-$ to 980 $cm^{-1}$ for the 18 $e^-$ $CF_3Mn(CO)_3(NO)^-$, whereas the symmetric C-F stretching bands overlap with each other within experimental uncertainties. Variations of the electron density and hybridization in the $\sigma$ donor orbital of the $CF_3$ ligand due to the different d orbital splittings of the complexes may be responsible for the distinctive C-F stretching frequencies observed in $CF_3Mn(CO)_5$ (18 $e^-$), $CF_3Mn(CO)_4^-$ (17 $e^-$), and $CF_3Mn(CO)_3(NO)^-$ (18 $e^-$).

Spectroscopic study of molecular ions has been of great experimental interest in recent years.[1-3] Various techniques have been employed to obtain information about the structures, vibrational and electronic spectra, and photodissociation dynamics of molecular ions.[2] Recent developments in high-resolution infrared spectroscopy made it possible to study the individual vibration-rotation levels of relatively simple ions such as $HD^+$, $HeH^+$, $CH^+$, and $H_3^+$.[2,3] However, there have been only a few experimental observations of infrared spectra of organometallic ions in the gas phase.

We have recently explored the technique of multiphoton dissociation[4] using a low-power $CO_2$ laser to obtain infrared fre-

(1) In *Gas Phase Ion Chemistry*; Bowers, M. T., Ed.; Academic Press: New York, 1984; Vol. 3.
(2) *Molecular Photodissociation Dynamics*; Ashfold, M. N. R., Baggott, J. E., Eds.; The Royal Society of Chemistry: London, 1987.
(3) *Molecular Ions: Spectroscopy, Structure, and Chemistry*; Miller, T. A., Bondybey, V. E., Eds.; North-Holland Publishing: Amsterdam, 1983.
(4) (a) Thorne, L. R.; Beauchamp, J. L. In *Gas Phase Ion Chemistry*; Bowers, M. T., Ed.; Academic Press: New York, 1984; Vol. 3, p 42 and earlier references therein. (b) Hanratty, M. A.; Paulsen, C. M.; Beauchamp, J. L. *J. Am. Chem. Soc.* **1985**, *107*, 5074. (c) Lupo, D. W.; Quack, M. *Chem. Rev.* **1987**, *87*, 181 and earlier references therein. (d) Watson, C. H.; Baykut, G.; Eyler, J. R. In *Fourier Transform Mass Spectrometry*; Buchanan, M. V. Ed.; American Chemical Society: Washington, DC, 1987; p 140. (e) Schulz, P. A.; Sudbo, A. S.; Krajnovich, D. J.; Kwok, H. S.; Shen, Y. R.; Lee, Y. T. *Annu. Rev. Phy. Chem.* **1979**, *30*, 379.

0002-7863/90/1512-2066$02.50/0 